



CHORUS

This is the accepted manuscript made available via CHORUS. The article has been published as:

Casimir torque on a cylindrical gear

Varun Vaidya

Phys. Rev. A **90**, 022105 — Published 7 August 2014

DOI: [10.1103/PhysRevA.90.022105](https://doi.org/10.1103/PhysRevA.90.022105)

The Casimir torque on a cylindrical gear

Varun Vaidya¹

¹*Department of Physics, Carnegie Mellon University, Pittsburgh, PA 15213*

We utilize Effective Field Theory(EFT) techniques to calculate the Casimir torque on a cylindrical gear in the presence of a polarizable but neutral object. We present results for the energy and torque as a function of angle for a gear with multiple cogs, as well as for the case of a concentric cylindrical gear.

I. INTRODUCTION

The Casimir force has been the subject of many research papers since the force between two polarizable atoms [1] was calculated by Casimir and Polder in 1948. Since then there has been a tremendous interest in this field involving the physical effects of this force in various geometrical configurations. The first calculation for the Casimir torque which is the angular analogue of the Casimir force was calculated in 1973 [2]. This was followed by a calculation for the Casimir torque between two uniaxial birefringent plates [3]. With the recent advancement in nanotechnology, there has been an interest in what are called non-contact gears to determine the torque between two corrugated concentric cylindrical surfaces. This was first proposed as a non contact, wear proof, rack and pinion arrangement which could be miniaturized to the nanometer scale [4]. This was then extended to the case of concentric corrugated cylinders [5]. As a first step based on this idea, the torque between two corrugated metal plates [6],[7] was calculated followed by a similar calculation for concentric corrugated metallic cylinders for the scalar field [8]. We consider the same geometrical arrangement with the exception that the cogs of the gear are made of a polarizable but neutral dielectric material instead of being metallic. This paper uses the world line Effective Field Theory(EFT) approach [10] to calculate the interaction energy between a cylindrical gear and a polarizable object. This technique is then extended to the case of a concentric cylindrical gear with dielectric cogs. The approach mirrors the work done in the context of membranes [11], [12].

II. CASIMIR TORQUE

We first consider the simple case of an infinitely long perfectly conducting(infinite conductivity at zero temperature) cylinder of radius a , with a single dielectric cog which we denote as A(fig.1). The cylinder is centered at the origin and is oriented along the z axis. We have a small polarizable object(B) at a distance r from the origin. Both A and B are neutral and isotropic. For simplicity, we define the z coordinates of A and B to be the same. The scale ΔE determines the typical gap between the ground state and first excited state of the cogs(A,B) which, of course, depends on the microscopic structure of the cogs. Thus, the relevant scales in the problem are:

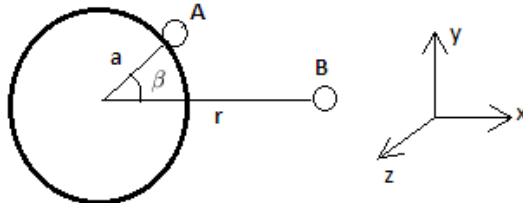


FIG. 1. Conducting cylindrical gear

The size of the cogs (R), the energy gap of the cogs (ΔE) and the distance between the cogs d . We will assume that $(1/\Delta E, R) \ll d$ so that we will be performing an expansion in $\lambda_1 \equiv R/d$ as well as $\lambda_2 \equiv 1/(\Delta E d)$. The expansion in λ_1 corresponds to the multipole expansion. On the other hand, the expansion in λ_2 controls the corrections arising from exciting the internal degrees of freedom of the cog. In other words, higher dimensional operators will be suppressed by powers of λ_2 which is equivalent to a systematic expansion in ω/ω_0 where ω controls the time dependence of the Electromagnetic field while ω_0 is the resonance frequency of the polarizability which depends on ΔE . We will be working at leading order in both these expansion parameters, though the corrections can be easily accounted for within the EFT formalism. Furthermore, we will consider the limit $\lambda_1 \gg \lambda_2$, so that the dominant corrections will come from the multipole expansion, though this is just a formality since we are working at leading order.

In the EFT formalism [10], one begins by integrating out the higher scales $(1/R, \Delta E)$, generating a series of higher dimensional operators whose coefficients can be determined by matching. In this way, the cogs are treated as point particles (A, B). These particles are taken to be static so that their world lines have no dynamical action. The finite size effects and frequency dependence of the polarizability are encoded in higher dimensional operators which reside on the world line and are constructed by writing down the lowest dimensional operators consistent with the relevant symmetries: Lorentz, gauge, and world line reparameterization invariance. At leading order in λ_1 and λ_2 , we have two operators [13], so that the action is given by:

$$S_{int} = \int d\tau \sum_{i=1}^2 (C_{b_i} \sqrt{v^2} F_{\mu\nu} F^{\mu\nu} + \frac{C_{e_i}}{\sqrt{v^2}} v^\mu F_{\mu\nu} v_\alpha F^{\alpha\nu}). \quad (1)$$

All the information about the internal structure of the cogs is absorbed in the couplings C_{e_i} and C_{b_i} which are determined via a matching procedure. By working at the level of the action, one can calculate in arbitrarily complicated geometries as long as the expansion in λ_1, λ_2 is well behaved. On the other hand, matching can be done in any simple physical process where the exact result, using the full microscopic theory, can be either calculated, if internal dynamics are understood, or measured otherwise. Matching tells us that the effective couplings C_{e_i} and C_{b_i} are related to the the electric and magnetic polarizabilities (α_{e_i}) and (α_{b_i}) respectively [10]. We consider only electric polarization, since both A and B are stationary such that

$$S_{int} = \int d\tau \sum_{i=1}^2 (-\alpha_{e_i} E^2). \quad (2)$$

The contribution of the magnetic polarizability is suppressed by the velocity of the internal constituents of the composite particles A and B. We employ the path integral approach to calculate the component of the Casimir interaction energy which contributes to the torque, via the relation

$$\langle 0 | e^{-iVT} | 0 \rangle = \int DA e^{i(S_0 + S_{int})}$$

Here S_0 is the action for the electromagnetic field in the presence of the cylinder without the perturbations, A and B. V is the total energy which includes both, the self energies of the cogs A and B, and their interaction energy. Out of these two contributions, only the interaction energy of A and B which depends on angle β [see Fig.1], contributes to the torque. The leading order contribution to the interaction energy is given by

$$\begin{aligned} V_{int} &= \frac{-i}{2T} \langle 0 | S_{int}^2 | 0 \rangle \\ &= \frac{-i}{T} (\alpha_{e_1} \alpha_{e_2}) \int d\tau_1 \int d\tau_2 \langle E^2(\vec{r}', \tau_1) E^2(\vec{r}, \tau_2) \rangle \end{aligned} \quad (3)$$

To calculate the energy we need the time ordered two point function(propagator) for each combination of components of the electric field in the presence of a conducting cylinder. We use the fact that the propagator is the Green's function for the equation of motion of the field, calculated in the Feynman prescription. This prescription is later used to perform a Wick rotation for evaluating the contour integral for the Green's function. Since we have a vector field, we then need to evaluate the

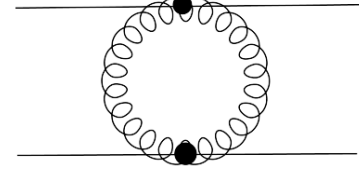


FIG. 2. Leading order Feynman diagram for V_{int} involving exchange of virtual photons between the two cogs. The dots represent the insertion of leading effective operator in the Lagrangian for the two cogs.

Green's dyadic (a 3x3 matrix) with the boundary conditions for the electromagnetic field at the surface of the conducting cylinder. This has already been calculated in [9] and is given by

$$i \langle E_i(\vec{r}', \tau_1) E_j(\vec{r}, \tau_2) \rangle = \int \frac{d\omega}{2\pi} e^{-i\omega(\tau_1 - \tau_2)} (\hat{i} \cdot \overleftrightarrow{\Gamma} \cdot \hat{j}) \quad (4)$$

where $i, j = \{r, \phi, z\}$.

$$\begin{aligned} \overleftrightarrow{\Gamma}(\omega, \vec{r}, \vec{r}') &= \sum_{m=-\infty}^{\infty} \int \frac{dk_z}{2\pi} [\mathbf{M}\mathbf{M}'^* F_m(r, r') \\ &+ \frac{1}{\omega^2} \mathbf{N}\mathbf{N}'^* G_m(r, r')] \chi_{mk_z}(\phi, z) \chi_{mk_z}^*(\phi', z') \end{aligned} \quad (5)$$

where the primed operators act on the primed coordinates.

$$\begin{aligned} \chi_{mk_z}(\phi, z) &= \frac{1}{\sqrt{2\pi}} e^{im\phi} e^{ik_z z} \\ \mathbf{M} &= \hat{r} \frac{im}{r} - \hat{\phi} \frac{\partial}{\partial r} \\ \mathbf{N} &= \hat{r} ik_z \frac{\partial}{\partial r} - \hat{\phi} \frac{mk_z}{r} - \hat{z} d_m \\ d_m &= \frac{1}{r} \frac{\partial}{\partial r} r \frac{\partial}{\partial r} - \frac{m^2}{r^2} \end{aligned}$$

For $r > r'$,

$$\begin{aligned} F_m(r, r') &= \frac{\omega^2 i\pi}{2k_\rho^2} H_m(k_\rho r) [J_m(k_\rho r') - \frac{J'_m(k_\rho a)}{H'_m(k_\rho a)} H_m(k_\rho r')] \\ &- \frac{1}{2|m|k_\rho^2} \left[\left(\frac{r'}{r}\right)^{|m|} + \frac{a^{2|m|}}{r^{|m|} r'^{|m|}} \right] \end{aligned}$$

$$\begin{aligned} G_m(r, r') &= \frac{\omega^2 i\pi}{2k_\rho^2} H_m(k_\rho r) [J_m(k_\rho r') - \frac{J_m(k_\rho a)}{H_m(k_\rho a)} H_m(k_\rho r')] \\ &- \frac{1}{2|m|k_\rho^2} \left[\left(\frac{r'}{r}\right)^{|m|} - \frac{a^{2|m|}}{r^{|m|} r'^{|m|}} \right] \end{aligned}$$

$$k_\rho = \sqrt{\omega^2 - k_z^2}$$

This is basically an expansion of the Green's function in vector cylindrical harmonics. Another equation that will aid in simplifying the calculation is the Wronskian for the Green's function.

$$J_m(k_\rho r)H'_m(k_\rho r) - J'_m(k_\rho r)H_m(k_\rho r) = \frac{2i}{\pi k_\rho r}$$

The coordinates of A and B are $\vec{r}' \equiv (a, \phi', z)$ and $\vec{r} \equiv (r, \phi, z)$ respectively. Since A is located on the surface of the cylinder, the boundary conditions imply that the components of the Green's dyadic that contribute to the energy are

$$V_{int} = \frac{-2i}{T} \alpha_{e_1} \alpha_{e_2} \int d\tau_1 \int d\tau_2 (< E_{r'}(\vec{r}', \tau_1) E_r(\vec{r}, \tau_2) >^2 + < E_{r'}(\vec{r}', \tau_1) E_\phi(\vec{r}, \tau_2) >^2 + < E_{r'}(\vec{r}', \tau_1) E_z(\vec{r}, \tau_2) >^2) \quad (6)$$

Evaluating each of the terms gives a fairly complicated expression for the interaction energy.

$$V_{int} = 2i(\alpha_{e_1} \alpha_{e_2}) \int \frac{d\omega}{2\pi} \int \frac{dk_{z_1}}{2\pi} \int \frac{dk_{z_2}}{2\pi} \sum_{m_1=-\infty}^{\infty} \sum_{m_2=-\infty}^{\infty} \frac{e^{im_1(\phi-\phi')}}{2\pi} \frac{e^{im_2(\phi-\phi')}}{2\pi} \quad (7)$$

$$\left[\frac{im_1 k_{z_1}^2}{k_{\rho_1}^2 a r} \frac{H_{m_1}(k_{\rho_1} r)}{H_{m_1}(k_{\rho_1} a)} - \frac{im_1 \omega^2}{k_{\rho_1}^2 a^2} \frac{H'_{m_1}(k_{\rho_1} r)}{H'_{m_1}(k_{\rho_1} a)} \right] \left[\frac{im_2 k_{z_2}^2}{k_{\rho_2}^2 a r} \frac{H_{m_2}(k_{\rho_2} r)}{H_{m_2}(k_{\rho_2} a)} - \frac{im_2 \omega^2}{k_{\rho_2}^2 a^2} \frac{H'_{m_2}(k_{\rho_2} r)}{H'_{m_2}(k_{\rho_2} a)} \right]$$

$$+ \left[\frac{k_{z_1}^2}{k_{\rho_1} a} \frac{H'_{m_1}(k_{\rho_1} r)}{H_{m_1}(k_{\rho_1} a)} - \frac{\omega^2 m_1^2}{k_{\rho_1}^3 a^2 r} \frac{H_{m_1}(k_{\rho_1} r)}{H'_{m_1}(k_{\rho_1} a)} \right] \left[\frac{k_{z_2}^2}{k_{\rho_2} a} \frac{H'_{m_2}(k_{\rho_2} r)}{H_{m_2}(k_{\rho_2} a)} - \frac{\omega^2 m_2^2}{k_{\rho_2}^3 a^2 r} \frac{H_{m_2}(k_{\rho_2} r)}{H'_{m_2}(k_{\rho_2} a)} \right]$$

with

$$k_{\rho_1} = \sqrt{\omega^2 - k_{z_1}^2}, \quad k_{\rho_2} = \sqrt{\omega^2 - k_{z_2}^2}.$$

The contour integral over ω is to be done using the Feynman prescription. This can be achieved by first doing a counterclockwise rotation in the complex ω plane effectively going to Euclidean space, which is essentially a Wick rotation.

Define $\eta = -i\omega$, $\lambda_j = -ik_{\rho_j}$ which gives $\lambda_j^2 = \eta^2 + k_{z_j}^2$

$$H_m(ix) = \frac{2}{\pi} \frac{1}{i^{m+1}} K_m(x)$$

Here $K_m(x)$ is the modified Bessel function of second kind. Defining $\beta = \phi - \phi'$ and $y = r/a$, and rescaling the integration variables, the final expression for the energy is given in terms of two terms with definite parity.

$$V_{int} = -2 \left(\frac{\alpha_{e_1} \alpha_{e_2}}{a^7} \right) \int \frac{d\eta}{2\pi} \int \frac{dk_{z_1}}{2\pi} \int \frac{dk_{z_2}}{2\pi} \sum_{m_1=-\infty}^{\infty} \sum_{m_2=-\infty}^{\infty} \frac{e^{i\beta(m_1+m_2)}}{4\pi^2} [-V_1(m_1, m_2) + V_2(m_1, m_2)] \quad (8)$$

$$V_1(m_1, m_2) = \left[\frac{m_1 k_{z_1}^2}{\lambda_1^2 y} \frac{K_{m_1}(\lambda_1 y)}{K_{m_1}(\lambda_1)} + \frac{m_1 \eta^2}{\lambda_1^2} \frac{K'_{m_1}(\lambda_1 y)}{K'_{m_1}(\lambda_1)} \right] \left[\frac{m_2 k_{z_2}^2}{\lambda_2^2 y} \frac{K_{m_2}(\lambda_2 y)}{K_{m_2}(\lambda_2)} + \frac{m_2 \eta^2}{\lambda_2^2} \frac{K'_{m_2}(\lambda_2 y)}{K'_{m_2}(\lambda_2)} \right]$$

$$V_2(m_1, m_2) = \left[\frac{k_{z_1}^2}{\lambda_1} \frac{K'_{m_1}(\lambda_1 y)}{K_{m_1}(\lambda_1)} + \frac{\eta^2 m_1^2}{\lambda_1^3 y} \frac{K_{m_1}(\lambda_1 y)}{K'_{m_1}(\lambda_1)} \right] \left[\frac{k_{z_2}^2}{\lambda_2} \frac{K'_{m_2}(\lambda_2 y)}{K_{m_2}(\lambda_2)} + \frac{\eta^2 m_2^2}{\lambda_2^3 y} \frac{K_{m_2}(\lambda_2 y)}{K'_{m_2}(\lambda_2)} \right]$$

For convenience we abbreviate the triple integral as

$$\int \frac{d\eta}{2\pi} \int \frac{dk_{z_1}}{2\pi} \int \frac{dk_{z_2}}{2\pi} \equiv \int d\zeta \quad (9)$$

Using the fact that $K_{m_1}(x) = K_{-m_1}(x)$, it is seen that V_1 is odd while V_2 is even in m_1 and m_2 . The even term V_2 contributes to an attractive force while the odd

terms gives a repulsive one. However, the magnitude of the V_1 is much smaller than V_2 , which still leads to a net attractive force.

$$V_{int} = \frac{\alpha_{e_1} \alpha_{e_2}}{a^7} F(y, \beta) \quad (10)$$

$F(y, \beta)$ is a dimensionless function of y and β .

$$T_1(y, \beta) = - \int \frac{d\zeta}{4\pi^2} \left[\sum_{m_1=-\infty}^{\infty} A_1(m_1, \lambda_1) \sum_{m_2=-\infty}^{\infty} A_2(m_2, \lambda_2) - \sum_{m_1=-\infty}^{\infty} B_1(m_1, \lambda_1) \sum_{m_2=-\infty}^{\infty} B_2(m_2, \lambda_2) + (m_1, \lambda_1) \leftrightarrow (m_2, \lambda_2) \right] \quad (12)$$

For $i = 1, 2$

$$A_1(m_i, \lambda_i) = m_i \sin(m_i \beta) v_2(m_i, \lambda_i) \quad (13)$$

$$A_2(m_i, \lambda_i) = \cos(m_i \beta) v_2(m_i, \lambda_i) \quad (14)$$

$$B_1(m_i, \lambda_i) = m_i \cos(m_i \beta) v_1(m_i, \lambda_i) \quad (15)$$

$$B_2(m_i, \lambda_i) = \sin(m_i \beta) v_1(m_i, \lambda_i) \quad (16)$$

$$v_1(m_i, \lambda_i) = \left[\frac{m_i k_{z_i}^2}{\lambda_i^2 y} \frac{K_{m_i}(\lambda_i y)}{K_{m_i}(\lambda_i)} + \frac{m_i \eta^2}{\lambda_i^2} \frac{K'_{m_i}(\lambda_i y)}{K'_{m_i}(\lambda_i)} \right] \quad (17)$$

$$v_2(m_i, \lambda_i) = \left[\frac{k_{z_i}^2}{\lambda_i} \frac{K'_{m_i}(\lambda_i y)}{K_{m_i}(\lambda_i)} + \frac{\eta^2 m_i^2}{\lambda_i^3 y} \frac{K_{m_i}(\lambda_i y)}{K'_{m_i}(\lambda_i)} \right] \quad (18)$$

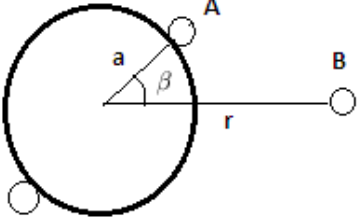


FIG. 3. Cylinder with two cogs

The same logic can be easily extended to the case when the cylinder has equally spaced (Fig.3) multiple cogs, again ignoring the self interaction energy of the cogs. At the same time, the interaction energy of any two cogs on the surface of the cylinder does not contribute to the torque. So the relevant energy is simply the interaction energy of the surface cogs with the off surface one.

III. CONCENTRIC GEAR

A similar procedure is followed in the case of a concentric gear. The simplest case is a gear with one cog as

Similarly, the torque is given by

$$\text{Torque} = \frac{\alpha_{e_1} \alpha_{e_2}}{a^7} T_1(y, \beta) \quad (11)$$

where we factor out a dimensionless function $T_1(y, \beta)$ from the total torque.

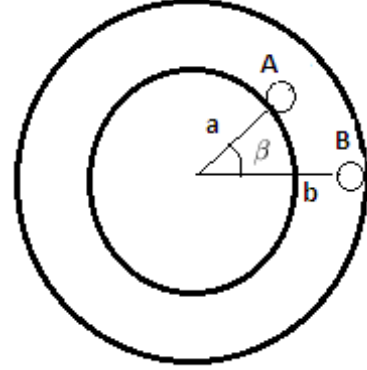


FIG. 4. Concentric cylindrical gear with a single cog.

shown in fig.(4), we have the outer conducting cylindrical shell (again of infinite conductivity) of radius b . The Green's dyadic is again of the same form with the functions F_m and G_m modified as follows.

For $r > r'$,

$$F_m(r, r') = \frac{\omega^2 i \pi}{2k_\rho^2} \left[\frac{J'_m(k_\rho a) J'_m(k_\rho b) H'_m(k_\rho a) H'_m(k_\rho b)}{J'_m(k_\rho b) H'_m(k_\rho a) - J'_m(k_\rho a) H'_m(k_\rho b)} \right] \\ \left[- \frac{J_m(k_\rho r) J_m(k_\rho r')}{J'_m(k_\rho a) J'_m(k_\rho b)} + \frac{J_m(k_\rho r) H_m(k_\rho r')}{J'_m(k_\rho a) H'_m(k_\rho b)} \right] \\ + \frac{H_m(k_\rho r) J_m(k_\rho r')}{H'_m(k_\rho a) J'_m(k_\rho b)} - \frac{H_m(k_\rho r) H_m(k_\rho r')}{H'_m(k_\rho a) H'_m(k_\rho b)} \right]$$

$$G_m(r, r') = \frac{\omega^2 i \pi}{2k_\rho^2} \left[\frac{J_m(k_\rho a) J_m(k_\rho b) H_m(k_\rho a) H_m(k_\rho b)}{J_m(k_\rho b) H_m(k_\rho a) - J_m(k_\rho a) H_m(k_\rho b)} \right] \\ \left[- \frac{J_m(k_\rho r) J_m(k_\rho r')}{J_m(k_\rho a) J_m(k_\rho b)} + \frac{J_m(k_\rho r) H_m(k_\rho r')}{J_m(k_\rho a) H_m(k_\rho b)} \right] \\ + \frac{H_m(k_\rho r) J_m(k_\rho r')}{H_m(k_\rho a) J_m(k_\rho b)} - \frac{H_m(k_\rho r) H_m(k_\rho r')}{H_m(k_\rho a) H_m(k_\rho b)} \right]$$

$$k_\rho = \sqrt{\omega^2 - k_z^2}$$

We have ignored the solutions to the homogeneous equation since they do not contribute to the physical observables. In this case, boundary conditions imply that only the $\langle E_r E_{r'} \rangle$ component of the dyadic will contribute to the torque. The final expression for the torque is again of the same form as Eqn.(11) evaluated using the modified Greens dyadic, with y now defined as b/a .

IV. NUMERICAL RESULTS AND ANALYSIS

We plot the dimensionless function T_1 Eqn.(12) for several values of y as a function of the angle β . The dimensionful torque can then be obtained from these plots by using Eqn.(11), inserting in the values of the dielectric polarization and the radius of the cylinder (a). In the numerical evaluation of T_1 , we have kept only a finite number of modes (m_1, m_2) of the functions V_1 and V_2 . To ascertain the numerical convergence of the series, we plot the T_1 for a gear with single cog Fig.5, for a value of $y=5$. In this plot we can clearly see the convergent nature of the series as higher modes are added.

Fig.7 plots T_1 for the same configuration with $y = 10$. It is clear from Eqn.12 that T_1 for a single cog satisfies the relations

$$T_1(-\beta) = -T_1(\beta) \quad (19)$$

$$T_1(\pi - \beta) = -T_1(\pi + \beta) \quad (20)$$

$$T_1(2\pi \pm \beta) = T_1(\pm\beta) \quad (21)$$

i.e the function T_1 is antisymmetric about $\beta = 0$ and $\beta = \pi$. So it is sufficient to plot T_1 for β in the range 0 to π . This can be easily extended to the case when we add N equally spaced cogs on the gear. Since the energy is a sum of the interaction energies of the individual cogs on the cylinder with the off surface cog, the torque for N cogs obeys a simple relation

$$T_N(\beta) = \sum_{n=0}^{N-1} T_1(\beta + 2n\pi/N) \quad (22)$$

At the same time, rotating the cylinder by $\frac{2\pi}{N}$ leaves the

system invariant, so that we get

$$T_N(\beta) = T_N(\beta + \frac{2\pi n}{N}) \quad (23)$$

for $n = 0, 1, \dots, N-1$.

Using these properties and the symmetries of T_1 , it can be proved that

$$T_N(n\pi/N - \beta) = -T_N(n\pi/N + \beta) \quad (24)$$

$$T_N(-n\pi/N - \beta) = -T_N(-n\pi/N + \beta) \quad (25)$$

for $n = 0, 1, \dots, N-1$.

In particular for $N = 2$, we can see that T_2 would be antisymmetric about $\beta = \pm\pi/2$ as seen in Fig. 8.

We can extend this analysis exactly to the case of the concentric gear. First consider the case of a single cog on both the inner and outer cylinders (Fig.4). We pull out a dimensionless factor T_1^c .

$$\text{Torque}^{\text{concentric}} = \frac{\alpha_{e1}\alpha_{e2}}{a^7} T_1^c(y, \beta) \quad (26)$$

Fig.9 which plots $T_1^c(y, \beta)$, again confirms the convergent nature of the series. Fig.10 shows the function $T_2^c(y, \beta)$ for the case of two equally spaced cogs both on the inner and outer cylinder of the gear. We can then define $T_N^c(y, \beta)$ for arbitrary N , which satisfies a similar relation as Eqn.(22).

$$T_N^c(\beta) = N \sum_{n=0}^{N-1} T_1^c(\beta + 2n\pi/N) \quad (27)$$

Given the convergent nature of the series, we can keep only a finite number of modes. This in turn implies that we can find a β sufficiently small such that $m\beta \ll 1$. Let us apply this approximation in Eqn.(8) for the case of a gear with a single cog. This gives an effective interaction energy for small angles as

$$V_{int} \approx \frac{1}{2} V \beta^2 \quad (28)$$

where

$$V(y) = \left(\frac{\alpha_{e1}\alpha_{e2}}{2a^7}\right) \int \frac{d\zeta}{4\pi^2} \sum_{m_1=-\infty}^{\infty} \sum_{m_2=-\infty}^{\infty} [(m_1^2 + m_2^2)v_2(m_1, \lambda_1)v_2(m_2, \lambda_2) - 2m_1m_2v_1(m_1, \lambda_1)v_1(m_2, \lambda_2)] \quad (29)$$

Not surprisingly, we get the potential for a harmonic oscillator since the potential has a minimum at $\beta = 0$. Defining

$$V(y) = \left(\frac{\alpha_{e1}\alpha_{e2}}{2a^7}\right) V_0(y) \quad (30)$$

we compute the dimensionless function V_0 for few values

of y , again retaining only the first six modes (TableI). The main utility of this computation is the fact that we can use V to exactly solve for the small angle dynamics of the system. The natural frequency of oscillations ω would be $\sqrt{V(y)/I}$, where I is the moment of inertia of the cylinder and cog.

TABLE I. Dimensionless function $V_0 = v * 10^{-4}$ for few values of y

y	5	6	7	8	9	10
v	0.3538	0.0642	0.0162	0.0051	0.0019	0.0008

We compute the dimensionful torque Eqn.(11) for a cylinder with one cog to get an idea of the magnitude of the torque involved. For the cogs, we can choose a dielectric nanoparticle such as one made from silica. For a case of a nanoparticle with high relative permittivity ($\gg 1$), the Clausius- Mossoti relation then gives us the polarizability (α) to be

$$\alpha = 3V \quad (31)$$

in natural units, where V is the volume of the nanoparticle. If we choose a spherical cog of radius 100 nm, it gives us a polarizability $\alpha = 1.2 * 10^{-20} m^3$. The bandgap for such dielectric nano particles is typically of the order of few eV. This corresponds to a distance of 100 nm. So, given the restrictions on the EFT used in this paper, we choose the distance between the cogs at $\beta = 0$ to be 1 μ m. This corresponds to a choice $\lambda_1 = \lambda_2 = 1/10$ for our power counting parameters. One of the cogs is placed on a cylinder made of a perfect conductor of radius 1 μ m. This gives us a value of $y=2$ for our computation. The torque in SI units is $1.5 * 10^{-24} * T_1(y = 2, \beta)$ Nm. Fig6 shows the dimensionless function T_1 for $y=2$ for a gear with a single cog($N=1$). This also reflects the feature of the series computation that the convergence of the series improves with increasing y , that is, as the distance between the cogs increases. Looking at the peak value of T_1 gives us a torque $0.3 * 10^{-24}$ Nm. The magnitude of the torque increases as the distance between the cogs is reduced which is seen from the Fig 6, Fig.5, Fig.7 as the value of y is reduced. Given a cog of a specific size, as the distance between the cogs is reduced, we need to include higher order terms in λ_1 . Similarly, given a specific bandgap (and hence the resonance frequency ω_0), we would need to include higher order operators in λ_2 . This would mean in general including operators with higher spatial and time derivatives of the electromagnetic field.

V. CONCLUSION

The effective field theory approach is an efficient way of calculating the interaction energy and subsequently the torque. We have obtained these results for the torque on a cylindrical gear and a concentric one in the regime where the size of the cogs is much smaller than the distance between them and the energy gap ΔE of the cogs is much greater than the inverse of the distance between the cogs. The main motivation for the EFT approach is that it allows a model independent way of calculating

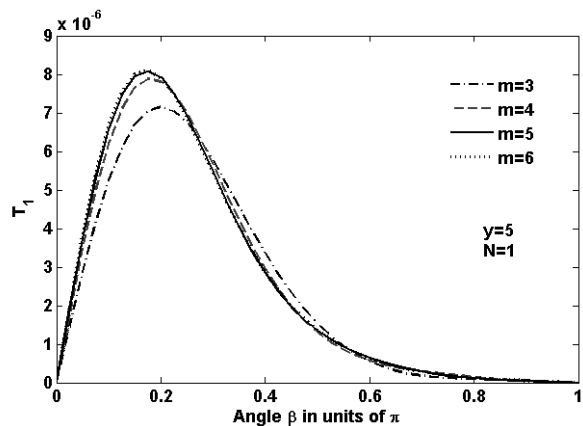


FIG. 5. Figure shows the effect of increasing the number of modes m in the computation of T_1 for a gear with a single cog($N=1$), $y=r/a=5$

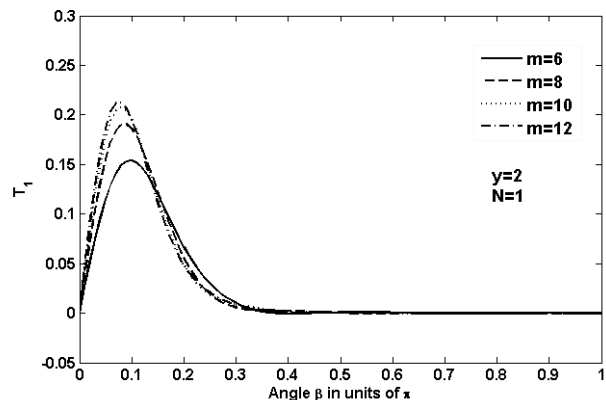


FIG. 6. Figure shows the effect of increasing the number of modes m in the computation of T_1 for a gear with a single cog($N=1$), $y=r/a=2$

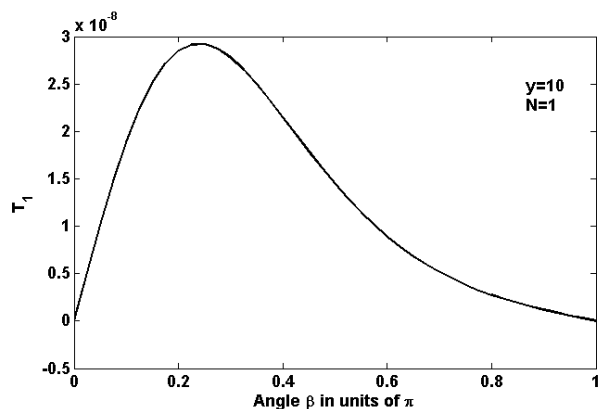


FIG. 7. T_1 for a gear with a single cog($N=1$) and $y=r/a=10$

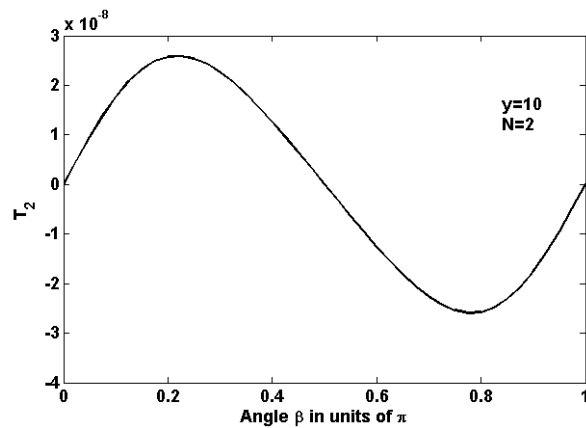


FIG. 8. T_2 for a two cog gear($N=2$), $y=r/a=10$

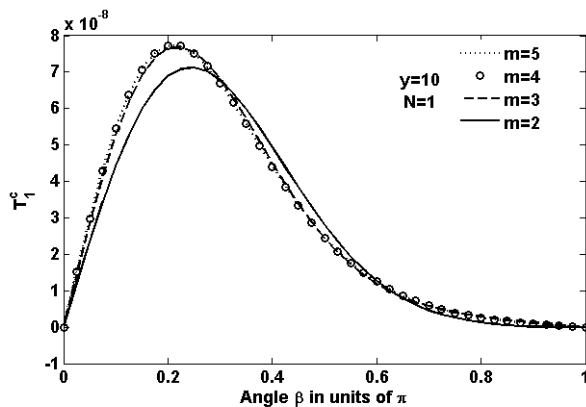


FIG. 9. T_1^c for a concentric gear with a single cog, $y=b/a=10$

the Casimir torque for gears, in the sense that all the information about the microscopic structure of the cogs appears in the form of Wilson coefficients of effective operators. This allows us to use this approach for virtually any type of material for the cog which satisfies the constraints of the EFT. The interaction energy that we have calculated is finite and leads to an attractive force and torque. The expression for the torque has been obtained

as an infinite series whose convergence has been numerically demonstrated. Numerical evidence suggests that the convergence of the series improves as the distance between the cogs increases. The analytic expression for the torque has been used to obtain symmetries obeyed by the expression for the torque for an N cog gear. The convergent nature of the series allows us to obtain a simple quadratic angle dependence for the interaction energy at small angles, which can be used to study the dynamics of the system in this regime. Finally, we have evaluated the torque for the specific case of a micrometer sized gear with nano cogs of high permittivity as an example of the magnitude of the torques involved. One must recall that we have assumed that the energy gap is greater than $1/r$. Should one wish to use this formalism where this condi-

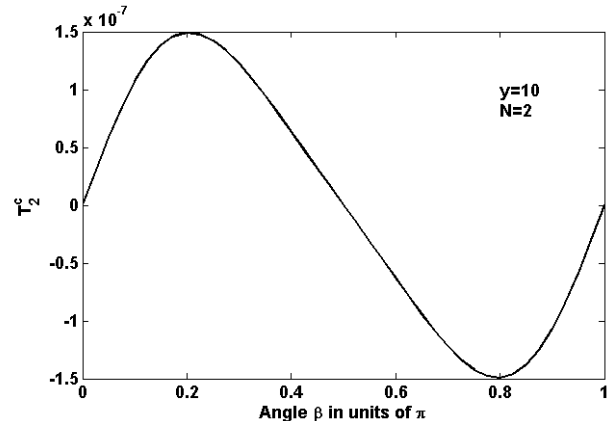


FIG. 10. T_2^c for a concentric gear with two cogs and $y=b/a=10$

tion is not met, then the theory must be augmented to allow for degrees of freedom to live on the cogs as in [17]. Further work in this area would be of interest.

VI. ACKNOWLEDGEMENTS

This work is supported by DOE contracts DOE-ER-40682-143 and DEACO2-C6H03000. I also thank Ira Rothstein for several discussions on the conceptual aspects of this project.

-
- [1] H. B. G. Casimir and D. Polder, Phys. Rev. **73**, 360 (1948).
 - [2] Yu. S. Barash, Izv. Vuzov, Ser. Radiofiz. 16, 1086 (1973) [Sov. Radiophys. **16**, 945 (1973)].
 - [3] S. J. van Enk, Phys. Rev. A **52**, 2569 (1995).
 - [4] A. Ashourvan, M.F. Miri, and R. Golestanian, Phys. Rev. Lett. **98**, 140801 (2007).
 - [5] F. C. Lombardo, F. D. Mazzitelli and P. I. Villar, J. Phys. A **41**, 164009 (2008)
 - [6] I. Cervero-Pelaez, K. A. Milton, P. Parashar and K. V. Shajesh, Phys. Rev. D **78**, 065018 (2008), arXiv:0805.2776 [hep-th].
 - [7] R. B. Rodrigues, P. A. Maia Neto, A. Lambrecht and S. Reynaud, Europhys. Lett. **76**, pp. 822828 (2006)
 - [8] Ines Cervero-Pelaez, Kimball A. Milton, Prachi Parashar, and K. V. Shajesh, Phys. Rev. D **78**, 065019 (2008).
 - [9] K. A. Milton, The Casimir Effect: Physical Manifestations of Zero-Point Energy, World Scientific, 2001.

- [10] W. D. Goldberger, I. Z. Rothstein, Phys. Rev. D **73**, 104029 (2006) [hep-th/0409156].
- [11] Cem Yolcu, I. Z. Rothstein, and Markus Deserno, Europhys. Lett. **96**, 20003 (2011).
- [12] I. Z. Rothstein, Nucl. Phys. B **862**, 576 (2012) [arXiv:1111.0533 [hep-th]].
- [13] C. R. Galley, A. K. Leibovich and I. Z. Rothstein, Phys. Rev. Lett. **105**, 094802 (2010) [arXiv:1005.2617 [gr-qc]].
C. R. Galley, A. K. Leibovich and I. Z. Rothstein, Phys. Rev. Lett. **109**, 029502 (2012) [arXiv:1206.4773 [gr-qc]].
- [14] H. B. G. Casimir, Proc. Kon. Ned. Akad. Wetensch. B **51**, 793 (1948)
- [15] Milton, Kimball A.; Deraad, Lester L., Jr.; Schwinger, Julian Annals of Physics, **115**, Issue 2, p.388-403 (1978)
- [16] Deraad, Lester L., Jr.; Milton, Kimball A. Annals of Physics, **136**, Issue 2, p.229-242 (1981)
- [17] W. D. Goldberger and I. Z. Rothstein, Phys. Rev. D **73**, 104030 (2006) [hep-th/0511133].